11586 *Inorg. Chem.* **2009**, *48*, 11586–11593
DOI: 10.1021/ic901422v

Inorganic Chemistry
Article

Anti-Mackay Polyicosahedral Clusters in La−Ni−Mg Ternary Compounds: Synthesis and Crystal Structure of the $La_{43}Ni_{17}Mg_5$ New Intermetallic Phase

Pavlo Solokha,*,† Serena De Negri,† Volodymyr Pavlyuk,‡,§ and Adriana Saccone†

†*Dipartimento di Chimica e Chimica Industriale, Università di Genova, Via Dodecaneso 31, I-16146 Genova, Italy,* ‡*Department of Inorganic Chemistry, Ivan Franko National University of Lviv, Kyryla and Mefodiya str. 6, 79005 Lviv, Ukraine, and* §*Institute of Chemistry and Environment Protection, Jan Dlugosz University, al. Armii Krajowej 13/15, 42200 Czestochowa, Poland*

Received July 21, 2009

The crystal structure of the complex $La_{43}Ni_{17}Mg_5$ ternary phase was solved and refined from X-ray single crystal diffraction data. It is characterized by a very large unit cell and represents a new structure type: $La_{43}Ni_{17}Mg_5$ − orthorhombic, *Cmcm*, *oS*260, a = 10.1895(3), b = 17.6044(14), c = 42.170(3) Å, Z = 4, $wR1$ = 0.0598, $wR2$ = 0.0897, 4157 F^2 values, 176 variables. The crystal structures of the La-rich La−Ni−Mg intermetallic phases La_4NiMg, $La_{23}Ni_7Mg_4$, and $La_{43}Ni_{17}Mg_5$ have been comparatively analyzed. The constitutive fragments of these structures are binary polyicosahedral core−shell clusters of Mg_4La_{22} and Mg_5La_{24} compositions together with binary polytetrahedral clusters of nickel and lanthanum atoms. The structures of the Mg−La clusters are described in detail as a unique feature of the analyzed intermetallic phases; the dodecahedral Voronoi polyhedra are proposed as a useful tool to characterize polyicosahedral clusters. The arrangements of the building units in the studied phases show some regularities; particularly the $i^4$3, $i^5$3 and *L*-i^4 units, made up of polyicosahedral clusters and analogous to the Kreiner i^3 and *L* units, are proposed as structural blocks.

1. Introduction

Among the intermetallic phases variety, complex crystal structures characterized by large unit cells and/or the presence of well-defined clusters, most often of icosahedral symmetry, are frequently related to atypical properties, including transport, mechanical, and chemical properties, which offer great potential for innovation.[1] Therefore a significant amount of research work is being done to discover new complex compounds in multicomponent alloys and to describe appropriately their crystal structure, which is of fundamental importance in addressing both chemical and physical properties of any system.

During our investigation of the La−Ni−Mg phase diagram the existence of three La-rich ternary phases was established.[2] The crystal structures of two of them, La_4NiMg and $La_{23}Ni_7Mg_4$, were subsequently published.[3,4] The crystal structure of $La_{43}Ni_{17}Mg_5$ was solved by means of single-crystal X-ray diffraction analysis, and it is presented in this paper. A crystallographic analysis of the three cited phases allowed to individuate as their building units core−shell Mg−La polyicosahedral clusters (PC) are very similar in all these structures, despite the fact that they correspond to three different crystalline systems.

A number of anti-Mackay clusters have been experimentally found in intermetallic phases. Smetana et al.[5,6] reported the existence of the Li_{19} one-component cluster, formed by two centered, interpenetrated icosahedra, in the binary compound $Ba_{19}Li_{44}$ and of the Li_{26} cluster, formed by four interpenetrated icosahedra, in the ternary compound $Li_{13}Na_{29}Ba_{19}$. A binary M26 polyicosahedral cluster of composition $Cu_{10}Zn_{16}$ is the fundamental building block of the cubic γ-brass structure (Cu_5Zn_8).[7] The *Bergman cluster*, consisting of 13 interpenetrating icosahedra, has been individuated in several phases both binary and ternary, such as Mg_2Zn_{11}, $Mg_2Al_5Cu_6$,[8,9] and $Mg_{32}(Al, Zn)_{49}$.[10]

*To whom the correspondence should be addressed. E-mail: solokha.pavlo@chimica.unige.it. Fax: +39-0103625051. Phone: +39-0103536159.

(1) *Basics of thermodynamics and phase transitions in complex intermetallics, Series on Complex Metallic Alloys-Vol. 1*; Belin-Ferrè, E., Ed.; World Scientific Publishing Co. Pte. Ltd.: Singapore, 2008.
(2) De Negri, S.; Giovannini, M.; Saccone, A. *J. Alloys Compd.* **2005**, *397*, 126.
(3) Tuncel, S.; Hermes, W.; Chevalier, B.; Rodewald, U. Ch.; Pöttgen, R. *Z. Anorg. Allg. Chem.* **2008**, *634*, 2140.
(4) Solokha P.; De Negri S.; Pavlyuk V.; Saccone A. *Chem. Met. Alloys*, in press.
(5) Smetana, V.; Babizhetskyy, V.; Vajenine, G. V.; Hoch, C.; Simon, A. *Inorg. Chem.* **2007**, *46*, 5425.
(6) Smetana, V.; Babizhetskyy, V.; Vajenine, G. V.; Simon, A. *Angew. Chem., Int. Ed.* **2006**, *45*, 6051.
(7) Gourdon, O.; Gout, D.; Williams, D. J.; Proffen, T.; Hobbs, S.; Miller, G. J. *Inorg. Chem.* **2007**, *46*, 251.
(8) Samson, S. *Acta Chem. Scand.* **1949**, *3*, 809.
(9) Samson, S. *Acta Chem. Scand.* **1949**, *3*, 835.
(10) Bergman, G.; Waugh, J. L. T.; Pauling, L. *Acta Crystallogr.* **1957**, *10*, 254.

 Published on Web 11/16/2009

However, to our knowledge, binary core−shell anti-Mackay polyicosahedral clusters were not previously found as constitutive fragments of ternary intermetallic phases. In this work the crystal structures of the La-rich La−Ni−Mg ternary phases are discussed with particular emphasis on the similarity of their constitutive units' structures, compositions, and packing modes.

2. Experimental Section

Synthesis. A sample of nominal composition $La_{66.7}Ni_{27.0}Mg_{6.3}$ was prepared from the elemental metals, all with nominal purities >99.9 wt %. Lanthanum and Nickel were supplied by Newmet Koch, Waltham Abbey, England, and Magnesium was supplied by MaTecK, Jülich, Germany.

An arc-sealed Ta-crucible containing stoichiometric amounts of the constituent elements was placed in an evacuated quartz vial, and then located in a resistance furnace equipped with a thermal cycle controller. The following thermal treatment was performed: (1) heating up to T = 850 °C (rate = 5 °C/min); (2) isothermal plateau (15 min); (3) cooling down to 350 °C (rate = 0.1 °C/min); (4) cooling down to room temperature (the furnace was switched off). After this treatment, the sample could easily be separated from the tantalum container. No side-reaction of the alloy with the crucible was detected.

Microstructure and Phase Analysis. Sample characterization was carried out by a scanning electron microscope (*EVO 40*, Carl Zeiss SMT Ltd., Cambridge, England) equipped with a Pentafet Link energy-dispersive X-ray spectroscopy (EDXS) system. Microstructure was observed and phase compositions measured. A smooth surface of the specimen was prepared by using SiC papers and diamond pastes down to 1 μm grain size. Cobalt standard was used for calibration. The obtained X-ray spectra were processed by the software package INCA Energy (Oxford Instruments, Analytical Ltd., Bucks, U.K.) for qualitative and quantitative analysis.

Single Crystal X-ray Diffraction and Structure Refinement. Intensity data collection was carried out on a $La_{43}Ni_{17}Mg_5$ single crystal extracted from the mechanically fragmented alloy which had the form of a compact ingot. The crystal was mounted on glass fibers using quick-drying glue. Data were collected at ambient conditions (295 K) on a four-circle diffractometer (Xcalibur Oxford Diffraction) equipped with a CCD detector by using the graphite monochromatized Mo Kα radiation (λ = 0.71073 Å). The instrument was operated in the ω scan mode. Intensity data were collected over the reciprocal space up to ~26° in θ and with exposures of 25 s per frame. Data integration, reduction, standard and analytical absorption corrections were made by CrysalisRed.[11] Unit cell parameters were refined from all the observed reflections [$I > 2\sigma(I)$].

Systematic absences analyses clearly indicate a base centered orthorhombic symmetry and the following plausible space groups: $Cmc2_1$ (no. 36), $C2cm$ (no. 40), and $Cmcm$ (no. 63). The structure solution was first tried in the centrosymmetric $Cmcm$ space group. The starting atomic parameters were deduced from an automatic interpretation of direct methods followed by difference Fourier syntheses using SHELX-97 package programs[12] yielding a starting model with 26 independent positions. Taking into account interatomic distances these positions were assumed to be 16 La, 7 Ni, and 3 Mg sites. This structure model refined by full-matrix least-squares on F^2 with isotropic displacements converged at R1 = 6.52% and wR2 = 9.96%. As any features indicating plausible non-centrosymmetricity (e.g., too short interatomic distances, elevated values of thermal displacement parameters, etc.) were obtained, this model was accepted as satisfying. To check for the correct composition, the occupancy parameters were varied in a separate series of least-squares cycles along with the displacement parameters. The occupancies did not vary noticeably and were always close to 100% for the La and Ni defined positions. In the Mg sites the occupancy values deviated up to 12%, but any attempt to refine Mg/La or Mg/Ni failed. Thus, in the final cycles the ideal composition was assumed again and refined with the anisotropic displacement parameters for all 26 atoms (convergence reached at R1 = 5.98% and wR2 = 8.97%, GOF = 1.179 with 176 parameters refined from 4157 independent reflections).

Table 1. Selected Crystallographic Data and Structure Refinement Parameters for $La_{43}Ni_{17}Mg_5$

empirical formula	$La_{43}Ni_{17}Mg_5$
EDXS composition	$La_{67.5}Ni_{25.8}Mg_{6.7}$
formula weight, g/mol	7092.75
radiation, wavelength, Å	Mo Kα, λ = 0.71073
crystal system	orthorhombic
space group, Z	$Cmcm$, 4
unit cell	
a (Å)	10.1895(3)
b (Å)	17.6044(14)
c (Å)	42.170(3)
V (Å^3)	7564.5(8)
density (ρ_{calc}), g/cm^3	6.23
abs. coeff. (μ), mm^{-1}	27.8
ref. data/params	4157/176
GOF on F^2	1.179
R1/wR2[13] [$I > 2\sigma(I)$]	0.0598/0.0897
(all data)	0.0840/0.0962
max. residual peaks (e/Å^3)	6.74/−3.43

The residual peaks in the final difference Fourier map of this strongly absorbing compound are somewhat high, the largest one is 6.7 e/Å^3 (1.03 Å from Mg2). However, this reasonably does not correspond to a real atom because the distances to the refined atoms positions are too short; the next highest residuals decrease smoothly (2.92 e/Å^3, 2.30 e/Å^3, 2.23 e/Å^3, etc.). The most probable explanation for the obtained residual peaks is a non-excellent quality of the single crystal which affects the quality of the diffraction data. In the resolution range from ~1.0 Å to infinity these residuals correlate well with the weakest observed reflections. The parallel refinement omitting these low-resolution reflections considerably decreases residual peaks (4.02 e/Å^3 and −1.54 e/Å^3) and converges at R1 = 3.69%, wR2 = 6.99%, and GOF = 1.090 for 2162 reflections. The relevant crystallographic details for the data refinement are listed in Table 1.

Table 2 contains refined positional parameters standardized by the Structure Tidy program.[14] The U_{eq} parameters and their corresponding standard deviation values are somewhat higher for Mg positions than for other atoms. This feature is common for rare earth rich R−Ni−Mg phases[3,15] and can therefore be assumed as an intrinsic property. Further details on the structure refinement can be found in the Supporting Information in the form of a CIF file. The CIF has also been deposited with Fachinformationszentrum Karlsruhe, 76344 Eggenstein-Leopoldshafen, Germany: depository numbers CSD-420642 ($La_{43}Mg_5Ni_{17}$).

3. Results and Discussion

3.1. SEM−EDXS Characterization. No impurity elements were detected in the sample. The measured gross

(11) *CrysalisRed, CCD data reduction GUI*, version 1.171.29.2; Oxford Diffraction: Abingdon, U.K., 2005.

(12) (a) Sheldrick G. M. *SHELXS−97: Program for the Solution of Crystal Structures*; University of Göttingen: Göttingen, Germany, 1997. (b) Sheldrick G. M. *SHELXL−97: Program for Crystal Structure Refinement*; University of Göttingen: Göttingen, Germany, 1997.

(13) R1 = $\sum||F_o| - |F_c||/\sum|F_o|$, wR2 = $[\sum w(F_o^2 - F_c^2)^2/\sum w(F_o^2)^2]^{1/2}$, and $w = 1/[\sigma^2F_o^2 + (AP)^2 + BP]$, $P = (F_o^2 + 2F_c^2)/3$. A and B are weight coefficients.

(14) Gelato, L.; Parthé, E. *J. Appl. Crystallogr.* **1987**, *20*, 139.

(15) Tuncel, S.; Roquefére, J.; Stan, C.; Bobet, J-L.; Chevalier, B.; Gaudin, E.; Hoffmann, R-D.; Rodewald, U.; Pöttgen, R. *Solid State Chem.* **2009**, *182*, 229.

Table 2. Atomic Coordinates and Equivalent Isotropic Displacement Parameters ($Å^2 \times 10^3$) for the $La_{43}Ni_{17}Mg_5$ Single Crystal

atom	Wyckoff position	site	*x*/*a*	*y*/*b*	*z*/*c*	U_{eq}[16]
La1	4*c*	*m*2*m*	0	0.38998(11)	1/4	15.3(4)
La2	8*g*	..*m*	0.18607(13)	0.20422(8)	1/4	15.2(3)
La3	8*f*	*m*..	0	0.13923(8)	0.17412(3)	14.4(3)
La4	16*h*	1	0.18828(9)	0.32898(5)	0.17400(2)	14.1(2)
La5	8*f*	*m*..	0	0.72780(7)	0.20648(3)	12.9(3)
La6	8*f*	*m*..	0	0.19723(8)	0.62632(3)	14.2(3)
La7	16*h*	1	0.19344(9)	0.20140(5)	0.10123(2)	13.9(2)
La8	16*h*	1	0.30731(9)	0.03499(5)	0.20655(2)	13.1(2)
La9	16*h*	1	0.30495(9)	0.49596(5)	0.12681(2)	14.2(2)
La10	16*h*	1	0.19578(9)	0.33018(5)	0.02600(2)	14.6(2)
La11	8*f*	*m*..	0	0.13880(8)	0.02884(3)	13.0(3)
La12	8*f*	*m*..	0	0.39065(8)	0.09880(3)	13.9(3)
La13	8*f*	*m*..	0	0.06788(8)	0.55569(3)	12.0(3)
La14	8*f*	*m*..	0	0.59876(8)	0.13280(3)	14.5(3)
La15	8*f*	*m*..	0	0.28079(9)	0.54761(4)	21.9(3)
La16	16*h*	1	0.31697(9)	0.03483(5)	0.04522(2)	14.4(2)
Ni1	8*f*	*m*..	0	0.07797(17)	0.09224(8)	18.2(7)
Ni2	8*f*	*m*..	0	0.45337(17)	0.16750(8)	18.4(7)
Ni3	16*h*	1	0.2812(2)	0.17213(12)	0.16828(5)	17.0(5)
Ni4	16*h*	1	0.2807(2)	0.35936(13)	0.09067(5)	18.3(5)
Ni5	4*c*	*m*2*m*	0	0.5987(3)	1/4	16.4(9)
Ni6	8*f*	*m*..	0	0.43146(19)	0.00910(8)	21.2(7)
Ni7	8*e*	2..	0.1275(3)	0	0	23.4(7)
Mg1	8*g*	..*m*	0.3338(10)	0.3774(5)	1/4	27.0(20)
Mg2	8*f*	*m*..	0	0.0678(5)	0.6912(3)	29.0(20)
Mg3	4*c*	*m*2*m*	0	0.0432(8)	1/4	26.0(30)

composition ($La_{66.9}Ni_{26.1}Mg_{7.0}$) corresponds to the nominal one. The alloy is near single phase ($La_{43}Ni_{17}Mg_5$ with composition 67.5 at % La, 25.8 at % Ni, 6.7 at % Mg); two secondary phases are present, in very small amounts (LaNi with composition 51.1 at % La, 48.9 at % Ni, and La_2Ni_2Mg with composition 43.6; at % La, 36.9 at % Ni, 19.5 at % Mg). The indicated phase compositions are values averaged on at least six EDXS measurements. A microstructure image is available in Supporting Information, Figure 1S.

3.2. Crystal Structure of $La_{43}Ni_{17}Mg_5$. The title compound represents a new structure type and possesses a quite large unit cell compared with the known orthorhombic intermetallic phases according to the Pearson's Crystal Data compilation.[17] The unit cell consists of 260 atoms occupying 26 Wyckoff sites.

The number of adjacent atoms in the structure agrees well with the sizes of the central atoms. The largest La atoms have 14, 15, or 16 neighbors at distances usual for intermetallic phases. The closest icosahedral arrangement around Mg atoms consists of 12 atoms: [$Mg1Mg_4La_8$], [$Mg2Mg_3La_9$], [$Mg3Mg_4La_8$]. The coordination sphere of the smallest Ni atoms contains always nine atoms in the form of equatorially tricapped trigonal prisms (in most cases exclusively La atoms surround Ni, only [$Ni6La_8Ni$] and [$Ni7La_8Ni$] containing one Ni atoms appear).

The compactness of this structure can be estimated from the average atomic volume contraction with respect to the sum of crystal volumes per formula unit of the constituents.[18] The calculated volume reduction of 0.35 $Å^3$/at. higher than those in La_4NiMg (0.17 $Å^3$/at.) and in $La_{23}Ni_7Mg_4$[3] (0.31 $Å^3$/at.), indicates a more compact structure. The interatomic distances analysis is reported below.

Because of the high lanthanum content, the nickel and magnesium atoms seem "isolated-like" being included in a La-framework; in fact, Mg−Ni distances (≥4.899 Å) exceed significantly the sum of metallic radii.[19] The interactions La−Mg (3.400−3.731 Å), Ni−Ni (2.532−2.598 Å), and Mg−Mg (3.154−3.387 Å) are close to the ideal single bond metallic radii sum. The 20% of the total number of La−La interactions are slightly shorter (≤3.735 Å) than those in the pure lanthanum hexagonal structure.[20] The major part of direct contacts between La and Ni atoms (2.857−3.100 Å) is closer rather to covalent radii sum (2.840 Å) than to metallic ones (3.123 Å).

3.3. Similar Features for Lanthanum Rich La−Ni−Mg Intermetallic Phases. 3.3.1. Anti-Mackay Core−Shell Mg−La Clusters in La-Rich La−Ni−Mg Intermetallic Phases. Despite the low Mg content in $La_{43}Ni_{17}Mg_5$ phase, the Mg atoms group in the form of isolated quasi regular Mg_5 trigonal bipyramids surrounded only by La atoms. This binary unit could be interpreted as a five icosahedra intergrown cluster of Mg_5La_{24} composition. A picture of this cluster is shown in Figure 1a (all the pictures were drawn with the DIAMOND[21] program), including dodecahedral Voronoi polyhedra representing the intergrown icosahedra.

It is known that a 13-atoms icosahedron can be considered to be made up of 20 tetrahedra sharing a common vertex; as a consequence, the Mg_5La_{24} polyicosahedral cluster consists of 67 tetrahedra, two of which are of Mg_4 composition (sharing a face they form the Mg_5 trigonal bipyramid) and other 65 of $MgLa_3$ composition. It has to

(16) U_{eq} is defined as one-third of the trace of the orthogonalized U_{ij} tensor.

(17) Villars, P.; Cenzual, K. *Pearson's Crystal Data, Release 2008*/*9*; ASM International: Ohio, U.S.A.

(18) $\Delta V_{at} = [V(La_xNi_yMg_z) - (x \times V(La) + y \times V(Ni) + z \times V(Mg))]/N$, where N is number of atoms in formula unit, V $(La_xNi_yMg_z) = V_{cell}$-$(La_xNi_yMg_z)/Z$.

(19) Emsley J. *The Elements*; Oxford University Press: Oxford, 1999.

(20) Bruzzone, G.; Merlo, F. *J. Less Comm. Met.* **1973**, *30*, 303.

(21) Brandenburg, K. *DIAMOND. Visual Crystal Structure Information System*, Version 2.0d.; Crystal Impact GbR: Bonn, Germany, 1998.

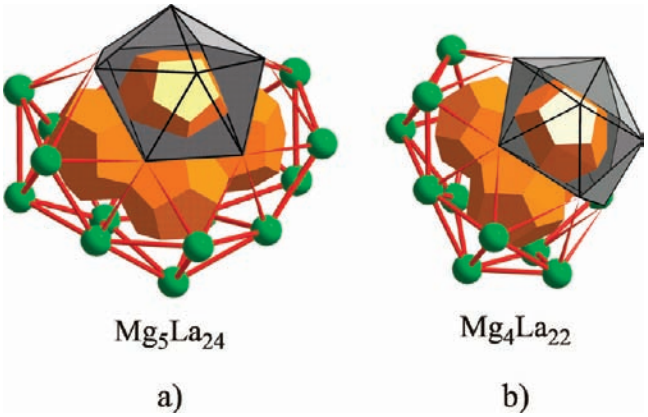

Figure 1. (a) Anti-Mackay Mg_5La_{24} polyicosahedral cluster in $La_{43}Ni_{17}Mg_5$. (b) Anti-Mackay Mg_4La_{22} polyicosahedral cluster in La_4NiMg and $La_{23}Ni_7Mg_4$ compounds. The outer part of a cluster icosahedral component is outlined in gray. Dodecahedra represent Voronoi polyhedra around central Mg atoms.

be noted that all tetrahedra are slightly distorted; however, because of the difference of the constituents' atomic dimensions, the strain energy is smaller with respect to a similar one-component cluster. All the La shell atoms are hexagonal close packed (*hcp*-like) with respect to the Mg_4 tetrahedron in the core, so that the Mg_5La_{24} unit can be classified as an anti-Mackay polyicosahedral cluster. All the Mg−Mg and Mg−La interatomic distances characterizing this polyicosahedral cluster are listed in Table 3. The volume of the Mg_5La_{24} PC, calculated by means of the 3DReshaper software,[22] is 376.1 Å^3, and the surface covered by shell La atoms[23] is 274.8 Å^2.

Similar Mg atoms arrangements can be outlined in the La_4NiMg and $La_{23}Ni_7Mg_4$ phases; in both structures the Mg atoms group in the form of Mg_4 regular tetrahedra surrounded by the same number of La atoms. This fragment of Mg_4La_{22} composition, similarly to the described Mg_5La_{24} PC, is formed by four intergrown icosahedra, and can therefore be viewed as an anti-Mackay polyicosahedral cluster (Figure 1b). The Mg_4La_{22} polyicosahedral cluster consists of 57 tetrahedra, one of which is of Mg_4 composition (it is the central tetrahedron) and other 56 of $MgLa_3$ composition. Interestingly, the volumes of the Mg_4La_{22} PC in the La_4NiMg (320.5 Å^3) and $La_{23}Ni_7Mg_4$ (323.1 Å^3) structures only differ by 0.8%. The Mg−Mg and Mg−La interatomic cluster distances (Supporting Information, Table S3) are close to those in the Mg_5La_{24}, reflecting the same building pattern and chemical bonding.

The stability of isolated clusters like those described above was predicted by Doye et al.[26] These authors introduced a global optimization approach which, applied to A_xB_y binary Lennard−Jones clusters, is able to search for the most stable composition and structure for a given cluster size. Applying this method to clusters up to 100 atoms and up to 30% difference in atom size the authors provide series of particularly stable cluster sizes (magic numbers) and structures, depending on the size ratio between the two types of atoms. For a size ratio equal to 1.15 (which is close to the size ratio between La and Mg $r_{La}/r_{Mg} = 1.17$) the first magic numbers 13, 19, 23, 26, 29, 34, and 45 correspond to anti-Mackay polyicosahedral clusters. The total numbers of atoms (26 and 29), the compositions (A_4B_{22} and A_5B_{24}), and the polyicosahedral structures of the studied clusters are in agreement with those reported by Doye et al.[26] among the particularly stable global minima. Moreover, the authors state that in this type of clusters the larger atoms (B) are preferentially located at the surface layer, leading to the formation of core−shell clusters; we observed these features in the two Mg_4La_{22} and Mg_5La_{24} PC, where smaller Mg atoms form the core and larger La atoms are situated in the shell.

The polyicosahedral clusters corresponding to the magic numbers listed above could be conveniently represented by means of the set of dodecahedral Voronoi polyhedra[27] around the central Mg atoms. While icosahedra are interpenetrated, the dodecahedral Voronoi polyhedra share some of their faces depending on the core atoms' number and arrangement. These polyhedra are therefore a useful and clear tool to imagine and construct polyicosahedral core−shell clusters consisting from 1 isolated icosahedron up to 13 intergrown icosahedra (which form the 45 atoms centered *Bergman cluster*,[10] whose core is a regular icosahedron). Several geometrical properties of the set of Voronoi polyhedra are directly connected with structural properties of the corresponding polyicosahedral cluster, particularly the number of core atoms in cluster corresponds to the total number of dodecahedra; the number of unique shell atoms (atoms which are not shared by neighboring icosahedra) is the total number of dodecahedra faces which do not share any edge; the number of shell atoms that are localized at the interface of icosahedra is the sum of the edges shared by only two pentagonal faces and of the common vertices of three adjacent pentagonal faces (because each interface shell atom corresponds to two or three adjacent pentagonal faces depending on the stacking mode); the total number of tetrahedra the cluster can be divided in corresponds to the total number of vertices of combined dodecahedra.

Particularly interesting is the 34 atoms cluster, formed by seven intergrown icosahedra, because its highest order symmetry element is a 5-fold symmetry axis as in an isolated icosahedron.

The fact that binary clusters exist in ternary compounds gave us reasons to check if the same clusters exist in binaries with rare earth and magnesium. In fact, any rare earth metal rich (> 50 at %) compound exists. So, we decided to verify if any binary phase exists where Mg is the bigger atom. The ratio between atom sizes of Mg and Pd is the same as for the La/Mg pair. What is more, the

(22) *3DReshaper 7.1, 3D modeling and Control Software from data measured with 3D scanners*; Technodigit: Lyons, France, 1997−2008.

(23) The number of triangular faces the shell of the polyicosahedral cluster could be divided in could be found by the equation: $t = 2N - 4$; where N is the number of the shell atoms.

(24) Atom types are differenced. Mg^a and Mg^e corresponds to apical or equatorial vertices of trigonal bipyramid in the cluster's core. La^i and La^{sh} are the unique and shared vertices of interpenetrated icosahedra.

(25) Bold data represent core atoms interatomic distances.

(26) Doye, J.; Meyer, L. *Phys. Rev. Lett.* **2005**, *95*, 063401.

(27) Ferro R.; Saccone A. In *Intermetallic Chemistry*; Cahn R. W., Ed.; Elsevier: Amsterdam, The Netherlands, 2008; Chapter 3.

Table 3. Selected Interatomic[25] Bond Distances in the Mg_5La_{24} Polyicosahedral Cluster

atoms[26]	dist. (Å) × no.	atoms	dist. (Å) × No.	atoms	dist. (Å) × No.	atoms	dist. (Å) × No.
$Mg1^e-Mg2^a$	3.154(12) × 4	$Mg2^a-La9^i$	3.547(10) × 4	$Mg1^e-La2^i$	3.400(9) × 2	$Mg3^e-La2^i$	3.410(12) × 2
$Mg3^e-Mg2^a$	3.157(14) × 2	$Mg2^a-La6^i$	3.561(11) × 2	$Mg1^e-La1^i$	3.408(10) × 2	$Mg3^e-La3^{sh}$	3.619(7) × 2
$Mg1^e-Mg3^e$	3.375(15) × 2	$Mg2^a-La5^{sh}$	3.659(9) × 2	$Mg1^e-La8^{sh}$	3.622(8) × 4	$Mg3^e-La8^{sh}$	3.631(1) × 4
$Mg1^e-Mg1^e$	3.387(14) × 1	$Mg2^a-La8^{sh}$	3.674(5) × 4	$Mg1^e-La5^{sh}$	3.629(8) × 4		
$Mg2^a-Mg2^a$	4.959(18) × 1	$Mg2^a-La3^{sh}$	3.715(9) × 2	$Mg1^e-La4^{sh}$	3.633(5) × 4		
		$Mg2^a-La4^{sh}$	3.731(5) × 4				
			Interatomic Distances between Shell La Atoms				
$La8^{sh}-La9^i$	3.618(1) × 4	$La1^i-La8^{sh}$	3.705(2) × 4	$La4^{sh}-La6^i$	3.787(1) × 4	$La1^i-La4^{sh}$	3.887(1) × 4
$La5^{sh}-La6^i$	3.629(2) × 2	$La2^i-La5^{sh}$	3.711(1) × 4	$La2^i-La2^i$	3.792(2) × 1	$La4^{sh}-La5^{sh}$	3.891(1) × 4
$La8^{sh}-La8^{sh}$	3.665(1) × 2	$La4^{sh}-La9^i$	3.744(1) × 4	$La4^{sh}-La8^{sh}$	3.878(1) × 4	$La3^{sh}-La2^i$	3.891(1) × 4
$La5^{sh}-La5^{sh}$	3.670(2) × 1	$La1^i-La2^i$	3.780(2) × 2	$La8^{sh}-La3^{sh}$	3.879(1) × 4	$La6^i-La9^i$	3.939(2) × 4
$La8^{sh}-La2^i$	3.709(2) × 4	$La3^{sh}-La9^i$	3.780(1) × 4	$La2^i-La4^{sh}$	3.885(1) × 4	$La9^i-La9^i$	3.975(1) × 2

Mg rich Mg_2Pd compound exists[28] and could be conveniently described as a space filling arrangement of Pd_4Mg_{22} core−shell PC clusters that have the same number of atoms and composition as Mg_4La_{22} PC (in the original paper the Pd_4Mg_{22} fragment was called a γ-brass cluster, taking into account only its number of atoms and geometrical form).

This fact indicates that some structural relation has to exist reflecting the similarity between the binary Mg_2Pd and the ternary La_4NiMg compounds and possibly highlighting the influence of the third smallest constituent (Ni) addition. The existence of a group-subgroup relation[29,30] between Mg_2Pd (Ti_2Ni structure type) and La_4NiMg structures was checked. The relations of the Wyckoff positions were checked with the aid of the computer program POWDER CELL.[31] The space group symmetry is lowered from $F4_1/d\bar{3}2/m$ to $F\bar{4}3m$ by a *translationengleiche* reduction of index 2 (t2). The symmetry reduction on passing from Mg_2Pd to La_4NiMg is caused by the loss of the $\bar{3}$ axis that makes one able to order the Pd position (32*e*) by different atoms. The resulting two 16-multiplicity positions (16*e*) are occupied by nickel and magnesium atoms (see scheme of Bärnighausen formalism in Supporting Information, Figure S3). The Mg atoms positions in the "parent" Mg_2Pd structure (48*f*; 16*c*) correspond to the rare earth atoms sites (24*g*, 24*f*; 16*e*) in La_4NiMg.

3.3.2. Ni Polytetrahedral Clusters in La-Rich La−Ni−Mg Intermetallic Phases. Analysis of the atomic environment around the smallest Ni atom in La_4NiMg, $La_{23}Ni_7Mg_4$, and $La_{43}Ni_{17}Mg_5$ structures shows that it is always the same and consists of 9 adjacent atoms in the form of a three-capped trigonal prism. We can define it as a polytetrahedral core−shell cluster that could be divided into 14 tetrahedra, all of them having a central nickel atom as a common vertex. The small size of Ni polytetrahedral cluster compared with those of Mg_4La_{22} and Mg_5La_{24} is appropriately explained by the bigger atom sizes ratio of shell and core atoms $r_{La}/r_{Ni} = 1.50$.

3.3.3. Arrangement of Mg- and Ni-Clusters in the Crystal Space of Studied Compounds. The arrangement of

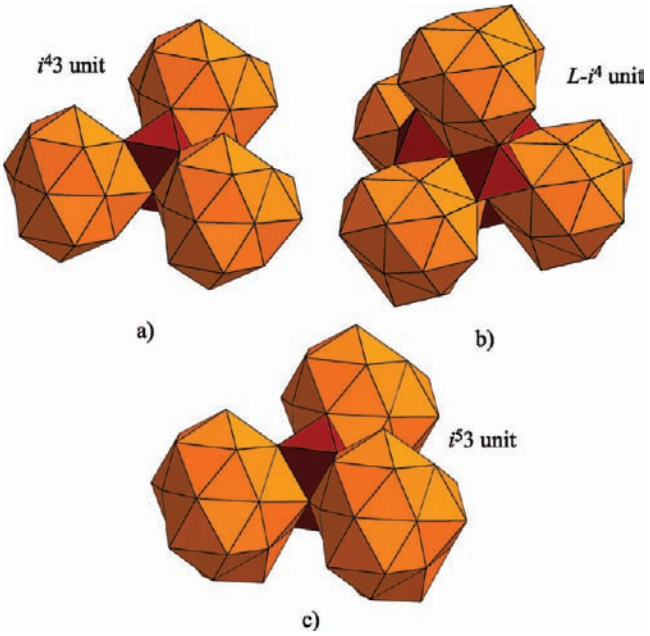

Figure 2. (a) $i^4$3 unit as a cluster of three Mg_4La_{22} PCs and two octahedra. (b) The L-i^4 unit as a cluster of five octahedra and four Mg_4La_{22} PCs around it. (c) The $i^5$3 unit as a cluster of two octahedra and three Mg_5La_{24} PCs.

Mg_4La_{22} and Mg_5La_{24} PC in the crystal space can be described by applying the idea of structure building units introduced by Kreiner et al.[32,33] to explain the crystal structure of numerous complex intermetallic phases and approximants for quasicrystals: these are the *i*3 unit (a cluster that contains three vertex connected icosahedra with overall local 3-fold symmetry) and the *L*-unit (a cluster of four vertex connected icosahedra). In the La_4NiMg crystal structure, three units Mg_4La_{22} PC are connected by their vertices in a manner similar to the *i*3 unit (it can be called an $i^4$3 unit). Note that the 3-fold axis of this unit lies along the 3-fold axes of the constituent Mg_4La_{22} PC. Moreover, the three-dimensional (3D) packing of Mg_4La_{22} PCs in La_4NiMg is realized analogically as in the Kreiner and Franzen *L*-unit together with the "pyrochlore unit" of five octahedra, and it can be defined as an L-i^4 unit (Figure 2a,b). In the $La_{23}Ni_7Mg_4$ structure only $i^4$3 units of the same shape and composition as in La_4NiMg could be found (crystal structure

(28) Makongo, J.; Prots, Yu.; Niewa, R.; Burkhardt, U.; Kreiner, G. *Z. Kristallogr. NCS* **2005**, *220*, 291.
(29) Bärnighausen, H. *MATCH, Commun. Math. Chem.* **1980**, *9*, 139.
(30) *International Tables for Crystallography, Vol. A1: Symmetry relations between space groups*; Wondratshek, H., Müller, U., Ed.; Kluwer Academic Publishers: Dordrecht, 2004.
(31) Nolze, G. *POWDER CELL. Computer program for the calculation of X-ray powder diagrams*; Bundesanstalt für Materialforschung: Berlin, Germany, 1996.
(32) Kreiner, G.; Franzen, H. *J. Alloys Compd.* **1995**, *221*, 15.
(33) Kreiner, G.; SchäPers, M. *J. Alloys Compd.* **1997**, *259*, 83.

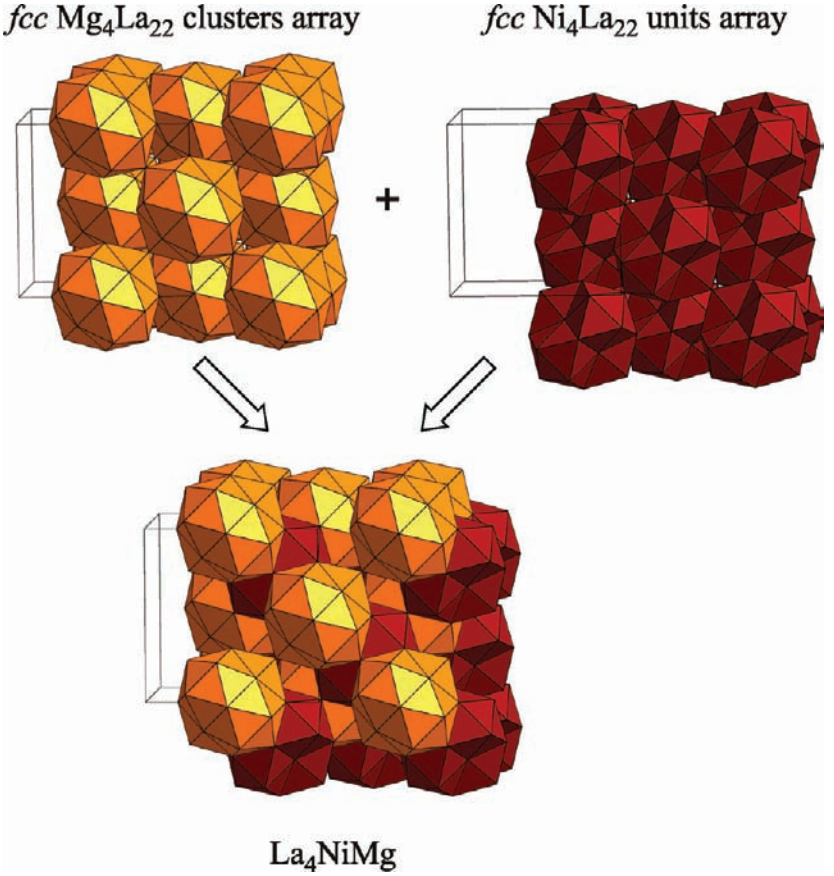

Figure 3. *fcc* arrays of Mg_4La_{22} PCs and Ni_4La_{22} units (four nickel cluster form) in La_4NiMg.

peculiarities would be discussed hereinafter). In the $La_{43}Ni_{17}Mg_5$ ternary compound another somewhat bigger $i^5$3 unit was singled out (Figure 2c). The 3-fold axis of this unit lies along the 3-fold axes of the constituent Mg_5La_{24} PC as in the previously described $i^4$3 unit.

The nickel clusters' arrangement in the crystal space is different for the studied ternary phases. In La_4NiMg, the highest symmetry and lowest Ni content compound, the 16*e* site occupied by Ni reflects in four groups of four nickel atoms in the form of regular tetrahedra (interatomic distances exceed single metal bond radii sum). Taking into account that each Ni atom is inside a $NiLa_9$ cluster, a 57 tetrahedra containing unit of tetrahedral symmetry could be singled out. It contains an empty La_4 tetrahedron in the center and other 56 $NiLa_3$ tetrahedra around it. This unit shares all vertices with four Mg_4La_{22} PCs which surround it. In the La_4NiMg space we can distinguish the *fcc* arrays of Mg_4La_{22} PCs and four nickel cluster units of general composition Ni_4La_{22} (Figure 3). The remaining space is filled by a framework of empty La octahedra, which was mentioned above and is known as a pyrochlore packing.[34]

With respect to La_4NiMg the $La_{23}Ni_7Mg_4$ compound contains a greater amount of Ni (20.6 at % at stoichiometric composition), which expresses in its crystal structure. The total number of Ni centered polytetrahedral clusters increases and they group in two similarly constructed units: the first is identical to the described Ni_4La_{22} unit of tetrahedral symmetry and the second one is a unit of three $NiLa_9$ clusters of Ni_3La_{19} composition with a 3-fold axis parallel to the [001] direction of the unit cell. As in La_4NiMg, in $La_{23}Ni_7Mg_4$ compound Mg_4La_{22} PCs are surrounded by four Ni containing units sharing all their vertices. Relative layers of Mg_4La_{22} PCs and Ni_4La_{22} units in La_4NiMg (perpendicular to [111] direction) and $La_{23}Ni_7Mg_4$ (perpendicular to [001] direction) are shown in Figure 4. In $La_{23}Ni_7Mg_4$ each of these layers is screwed at 60° relative to the successive ones, instead in La_4NiMg they are packed in cubic close packing mode.

The $La_{43}Ni_{17}Mg_5$ is the Ni richest phase in the La-rich corner of the La−Ni−Mg diagram (26.15 at % Ni). It is distinctive that, similarly to the common Mg behavior of forming PCs, Ni atoms also keep their tendency to form polytetrahedral clusters in the analyzed phases. Besides the presence of $NiLa_9$ clusters identical to those described for La_4NiMg and $La_{23}Ni_7Mg_4$ IMC, in the $La_{43}Ni_{17}Mg_5$ structure $NiLa_8Ni$ clusters (always in the form of a three-capped trigonal prism) were found. Two such clusters are intergrown forming the Ni_2La_{11} unit (note that identical units could be singled out in the La_2Ni_2Mg structure[35]). Other constructive polythetrahedral Ni cluster units are Ni_7La_{35} and Ni_3La_{19} (Figure 5). Similarly to the phases described above, in the $La_{43}Ni_{17}Mg_5$ structure the Ni_7La_{35} and Ni_3La_{19} units are gathered around the Mg_5La_{24} PCs (which always share all their vertices).

(34) Lord E.; Mackay A.; Ranganathan S. *New Geometries for New Materials*; Cambridge University Press: New York, 2006.

(35) Hoffmann, R. D.; Fugmann, A.; Rodewald, U. C.; Pöttgen, R. *Z. Anorg. Allg. Chem.* **2000**, *626*, 1733.

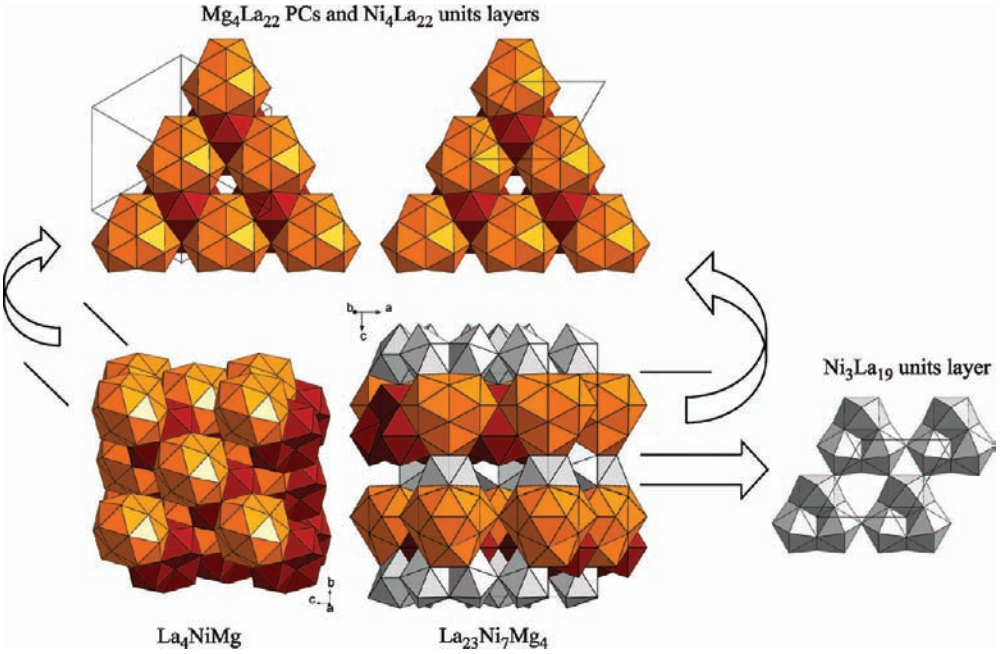

Figure 4. La_4NiMg and $La_{23}Ni_7Mg_4$ as complex structures with similar structural features: the identical Mg_4La_{22} PCs and Ni_4La_{22} units layers are outlined together with Ni_3La_{19} units layer, a special feature of $La_{23}Ni_7Mg_4$ IMC.

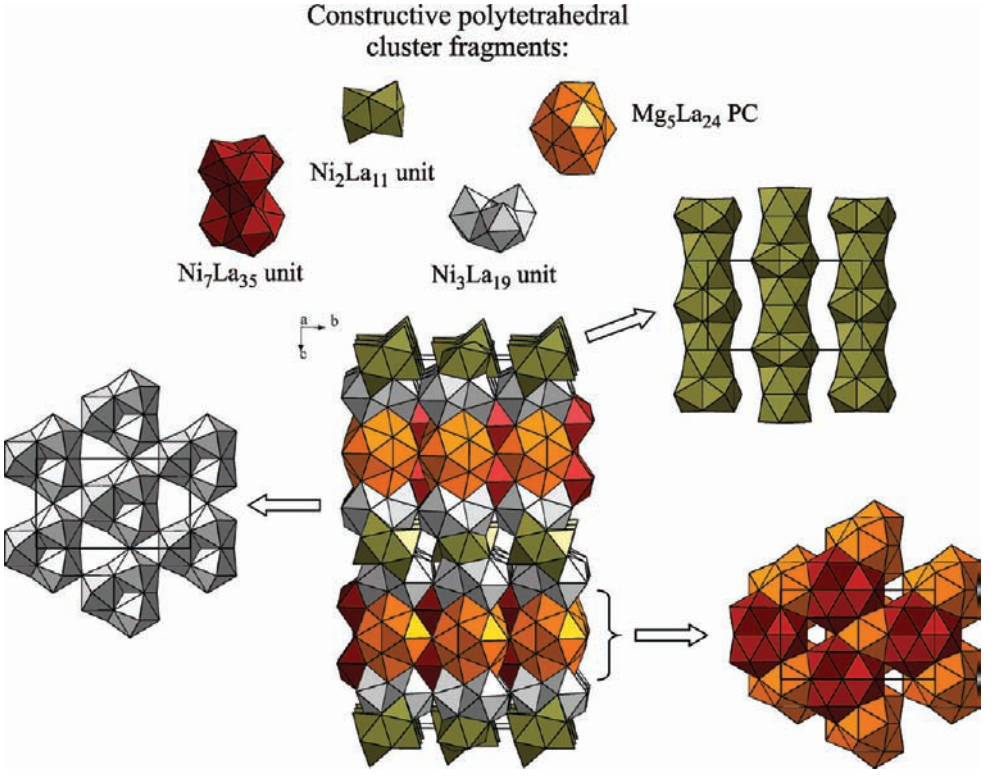

Figure 5. Crystal structure of complex $La_{43}Ni_{17}Mg_5$ compound. The constructive polytetrahedral cluster fragments together with respective layers they form are shown.

Along the [001] direction three different layers of building polytetrahedral units can be outlined (Figure 5).

The first layer, which distinguishes $La_{43}Ni_{17}Mg_5$ from the neighboring compounds, is a sequence of identical columns (each one shifted at $a/2$ with respect to the adjacent one) which in turn are linkages of Ni_2La_{11} units arranged along the [100] direction in a way that equally oriented blocks are alternated. The second layer is identical to the Ni_3La_{19} units layer in $La_{23}Ni_7Mg_4$. Finally, the third layer is an arrangement of Mg_5La_{24} PCs and Ni_7La_{35} units.

It is interesting that a similar Ni behavior can be outlined in binary La-rich La−Ni binary phases such as La_7Ni_3 and La_3Ni, characterized by significant volume contraction values (0.69 and 0.35 $Å^3$/at, respectively). In fact, the crystal space of these compounds is filled by Ni

polytetrahedral cluster units of formula $NiLa_9$. In the hexagonal La_7Ni_3 the two layers formed by Ni_3La_{19} units, identical to those in $La_{23}Ni_7Mg_4$ and $La_{43}Ni_{17}Mg_5$ IMCs, are intergrown alternatively along the [001] direction. In the orthorhombic La_3Ni, $NiLa_9$ clusters form layers with zigzag columns sharing their faces with the neighboring ones. Within a layer such columns share vertices among themselves.

4. Conclusions

In this work we have presented the crystal structure determination of the complex intermetallic phase $La_{43}Ni_{17}Mg_5$, which is characterized by a very large orthorhombic unit cell. A comparative analysis of the crystal structures of the La_4NiMg, $La_{23}Ni_7Mg_4$, and $La_{43}Ni_{17}Mg_5$ phases highlighted that they are fullfilled by bigger Mg−La and smaller Ni−La core−shell polytetrahedral binary clusters. Whereas these Ni-centered clusters are common for ternary and binary intermetallic phases, the Mg−La ones can be considered as a distinctive feature of the studied complex metallic alloys. The structure of these Mg (core)−La (shell) clusters, whose composition is Mg_4La_{22} or Mg_5La_{24}, allows them to be classified as anti-Mackay polyicosahedral clusters. The size, composition, and structure of the singled out clusters correspond to particularly stable global minima (magic numbers) calculated in the literature for Lennard−Jones isolated clusters. The arrangement of the Mg−La clusters in the crystal space can be described by means of building units (called here $i^4$3, $i^5$3, and L-i^4) analogous to the Kreiner i3 and L units, reflecting the complexity of the analyzed phases.

In this work we also started to analyze the cluster volumes and the volume contractions of these phases as keys to understanding their chemical bonding. For this purpose a comparative analysis of the numerous rare earth-rich R−Ni−Mg ternary phases already known is the object of our future research.

Supporting Information Available: X-ray crystallographic file in CIF format, back scattered electron image of alloy surface (Figure S1); unit cell projections together with coordination polyhedra of all the atoms in $La_{43}Ni_{17}Mg_5$ (Figure S2); group-subgroup relation in the Bärnighausen formalism for the Mg_2Pd (Ti_2Ni type) and La_4NiMg (Gd_4RhIn type) structures (Figure S3); anisotropic displacement parameters for $La_{43}Ni_{17}Mg_5$ (table S1), interatomic distances for $La_{43}Ni_{17}Mg_5$ (Table S2); interatomic distances for PCs in La_4NiMg and $La_{23}Ni_7Mg_4$ (Table S3). This material is available free of charge via the Internet at http://pubs.acs.org.